The photoinduced Ti^{3+} centre in $SrTiO_3$

2002 J. Phys.: Condens. Matter 14 13813

(http://iopscience.iop.org/0953-8984/14/50/308)

INSTITUTE OF PHYSICS PUBLISHING JOURNAL OF PHYSICS: CONDENSED MATTER

J. Phys.: Condens. Matter **14** (2002) 13813–13825 PII: S0953-8984(02)54384-8

The photoinduced Ti^{3+} centre in $SrTiO_3$

V V Laguta[1], M D Glinchuk[1], R O Kuzian[1], S N Nokhrin[1], I P Bykov[1], J Rosa[2], L Jastrabík[2] and M G Karkut[3]

[1] Institute for Problems of Material Science, Ukrainian Academy of Sciences, Krjijanovskogo 3, 03180 Kiev, Ukraine
[2] Institute of Physics, Academy of Sciences of the Czech Republic, Cukrovarnická 10, 16253 Prague, Czech Republic
[3] Laboratory of Condensed Matter Physics, University of Picardy, 33 rue Saint-Leu, 80039, Amiens, France

Received 7 October 2002
Published 6 December 2002
Online at stacks.iop.org/JPhysCM/14/13813

Abstract

We report the results of an electron spin resonance study of Ti^{3+} centres in $SrTiO_3$ single crystals. The Ti^{3+} centres are created in perturbed regular Ti^{4+} sites by trapping a photoelectron from the conduction band after ultraviolet irradiation of the sample at low temperature ($T < 180$ K). The centres are stable below ∼180 K. To our knowledge this is the first observation of such Ti^{3+} defects in a $SrTiO_3$ lattice.

At $T > T_c$ ($T_c \approx 105$ K corresponds to the temperature of the cubic–tetragonal phase transition), the Ti^{3+} centre exhibits an orthorhombic symmetry of the g-tensor with its principal axes oriented exactly along ⟨001⟩ and ⟨110⟩ crystal directions: $g[110] = 1.9920$, $g[1\bar{1}0] = 1.9375$, $g[001] = 1.8843$.

At $T < T_c$, due to a structural phase transition, two of the Ti^{3+} principal axes are tilted relative to the ⟨110⟩ directions by up to ±8° in the (001) crystal plane. The spectroscopic data are explained assuming Jahn–Teller orthorhombic distortions of the oxygen octahedron with non-linear $T_{2g} \times (e_g + t_{2g})$ vibronic coupling.

1. Introduction

During the past few decades, electron spin resonance (ESR) investigations of charge states and their changes due to light illumination, as well as the structure of intrinsic and extrinsic defects in perovskite-type oxides, have attracted a lot of attention. Apart from producing local structural information related to phase transitions, ESR investigation provides a basis for a deeper understanding of the microscopic mechanisms of photochromic, photorefractive, and photoconductive phenomena. There was extensive work devoted to the study of impurity ion states in the perovskite crystals $BaTiO_3$ [1], $PbTiO_3$ [2], and $SrTiO_3$ [3–5]. Among the ions, transition-metal impurity ions (for instance, iron and chromium ones) were the most frequently studied, and their states as well as their changes due to light illumination were studied in detail.

The study of light-induced intrinsic defects is of special interest. After the crystal is illuminated with photons of energies close to or greater than the energy gap, electrons can leave the valence band and be trapped by titanium ions, thereby creating different types of Ti^{3+} centre. Paramagnetic centres in $PbTiO_3$ and $BaTiO_3$, where an electron is trapped on a titanium ion nearest to an oxygen vacancy and/or a defect on a neighbouring A- or B-site, were studied in [1, 2, 6]. However, for a long time these centres were not observed in $SrTiO_3$. Only the ESR spectra arising from anti-site Ti^{3+} ions on Sr^{2+} sites have been reported for $SrTiO_3$ [7, 8].

In this paper we report on Ti^{3+} centres of another type in $SrTiO_3$ crystals, namely those originating from in-site-position Ti ions slightly perturbed by unidentified defects in the vicinity. First, we present the temperature behaviour of both electron-and hole-type paramagnetic centres created by ultraviolet (UV) illumination at 10 K. Then the main attention is given to the Ti^{3+} centre, for which the ESR spectra were studied in the temperature interval 20–160 K. On the basis of these studies, the structural and energetical properties of the Ti^{3+} centre are derived. The final section is devoted to an interpretation of the g-tensor in the framework of the orthorhombic $T_{2g} \times (e_g + t_{2g})$ Jahn–Teller distortion of an oxygen octahedron.

2. Samples and experimental details

The measurements were performed on nominally pure single-crystal samples of $SrTiO_3$ grown by the flame–fusion method. X-ray fluorescence analysis showed unwanted impurities at a level below 2 ppm except Al, Ba, and Ca which were present in the concentrations of 10, 14, and 19 ppm, respectively. The sample dimensions were $3 \times 2 \times 0.2$ mm^3, with the surfaces parallel to crystallographic (001) planes.

ESR spectra were recorded in the X-band microwave region. An Oxford instruments ESR-9 cryosystem allowed us to perform measurements in the temperature range 4.2–290 K with accuracy of 0.1–0.2 K. An arc lamp was used for optical irradiation of the samples.

3. Experimental results and their interpretation

3.1. Photoinduced spectra

Before light illumination, only a small signal from Fe^{3+} (with both cubic and axial symmetry) and Cr^{3+} centres was observed. After illumination by light with $\lambda = 365$ nm at $T = 10$–15 K, other strong ESR signals appeared (see figure 1(a)). The spectrum observed in the magnetic field 320–330 mT has already been ascribed to the O^-–Fe^{2+} hole centre [9]. The spectrum at $B = 330$–350 mT is new and, as we will demonstrate below, it arises from the Ti^{3+} ions. Due to the temperature dependence of the spin–lattice relaxation, the Ti^{3+} spectrum becomes much more intense at $T = 50$–60 K (figure 1(b)).

O^-–Fe^{2+} centres are thermally stable only to 20–22 K. Above this temperature, holes retrap to the O^- centre of an unknown structure, most probably that previously called I_1 [10] (figure 1(b)). Parts of the holes, freed from O^-–Fe^{2+} centres, recombine with electrons, localized at Ti^{3+}, thus decreasing the Ti^{3+} spectrum intensity (figure 2). Since to our knowledge the ESR parameters of the I_1 centre have not been published yet, table 1 presents the spin Hamiltonian parameters of the centre derived from angular dependences of the resonance fields. Heating the crystal up to 60–70 K, the holes were also freed from I_1 and were at least partially trapped by the Fe^{3+} impurity, creating the Fe^{5+} centre [11]. It can be clearly seen (figures 1(c) and 2) that when the Fe^{5+} ions are created, the intensity of the Fe^{3+} spectrum decreases. The remaining parts of the holes could recombine with localized electrons at Ti^{3+}.

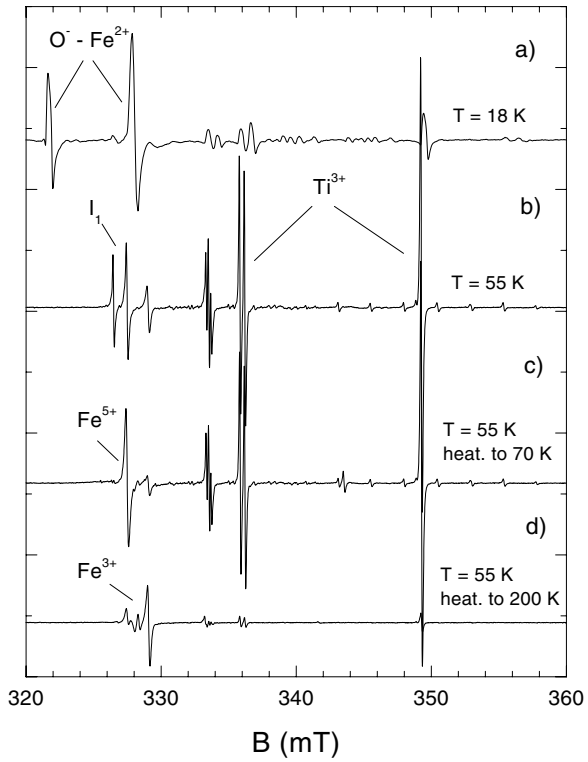

Figure 1. Ti^{3+} ESR spectra for $SrTiO_3$ for $B \parallel [001]$ at $T = 18$ K (a) and 55 K (b), (c), (d) produced by UV irradiation at $T = 10$ K; (c) and (d): spectra after pulsed heating to 70 and 200 K, respectively.

Table 1. Spin Hamiltonian parameters for O^- (I_1) centres in $SrTiO_3$. The orientation of the principal axes is given by the polar and azimuthal angles for one of the six equivalent O^- centres. All angles are given with respect to the cubic ⟨100⟩ directions.

	Polar and azimuthal angles of axes		Euler angles		
g-tensor	θ	φ	α	β	γ
g_1: 2.0188(1)	82	10	270	45	102
g_2: 2.0073(1)	45	108	180	45	102
g_3: 2.0161(1)	45	270	90	45	102
			0	45	102
			135	90	192
			225	90	192

Finally, at $T > 185$ K, electrons freed from the Ti^{3+} and at least partially recombined with holes at Fe^{5+} give rise to the Fe^{3+} spectrum (figure 1(d)). The data on the thermal stability of all observed centres are collected in figure 2.

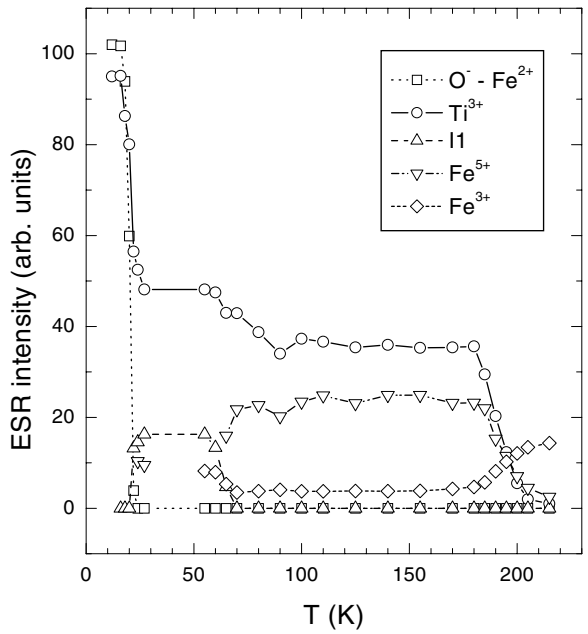

Figure 2. The temperature dependence of the ESR intensity of photoinduced centres created in $SrTiO_3$ by UV irradiation at $T = 10$ K.

Table 2. Spin Hamiltonian parameters of Ti^{3+} centres in $SrTiO_3$.

T (K)	g-factor	τ (deg)	$A(^{47,49}\mathrm{Ti})$ (10^{-4} cm^{-1})
57	$g_{[110]+\tau} = 1.9943(1)$	± 8	9.3(1)
	$g_{[1\bar{1}0]+\tau} = 1.9383(1)$		20.9(1)
	$g_{[001]} = 1.8871(1)$		21.31(2)
105	$g_{[110]} = 1.9920(2)$	0	—
	$g_{[1\bar{1}0]} = 1.9375(2)$		
	$g_{[001]} = 1.8843(2)$		

3.2. ESR spectra of Ti^{3+}

The present paper focuses on the Ti^{3+} centre, which has not been observed previously. The observed angular dependences of the resonance fields for a magnetic field rotating in the (001) plane (all angular dependences and directions are given relative to pseudo-cubic axes of the crystal) at $T = 55$ and 105 K are displayed in figure 3. From this polar plot it follows quite clearly that the ESR spectra relate to paramagnetic centres with a local orthorhombic symmetry. The magnetic resonance fields are described by a spin Hamiltonian in the following form:

$$\hat{H} = \beta \hat{S} g \overline{B} + \hat{S} A \hat{I}_1 + \hat{S} A \hat{I}_2 \tag{1}$$

where $S = 1/2$, $I_1 = 5/2$, and $I_2 = 7/2$. Principal values as well as orientations of the principal axes of the g-tensor and hyperfine tensor are listed in table 2.

The expected hyperfine structure observed for the line with $g = 1.8868$ is shown in figure 4. This hyperfine structure relates to the Ti isotopes: ^{47}Ti (nuclear spin $I = 5/2$, natural abundance -7.75%) and ^{49}Ti (nuclear spin $I = 7/2$, natural abundance -5.51%). Since the values of their magnetic moments are very close to each other, the hyperfine lines of ^{47}Ti

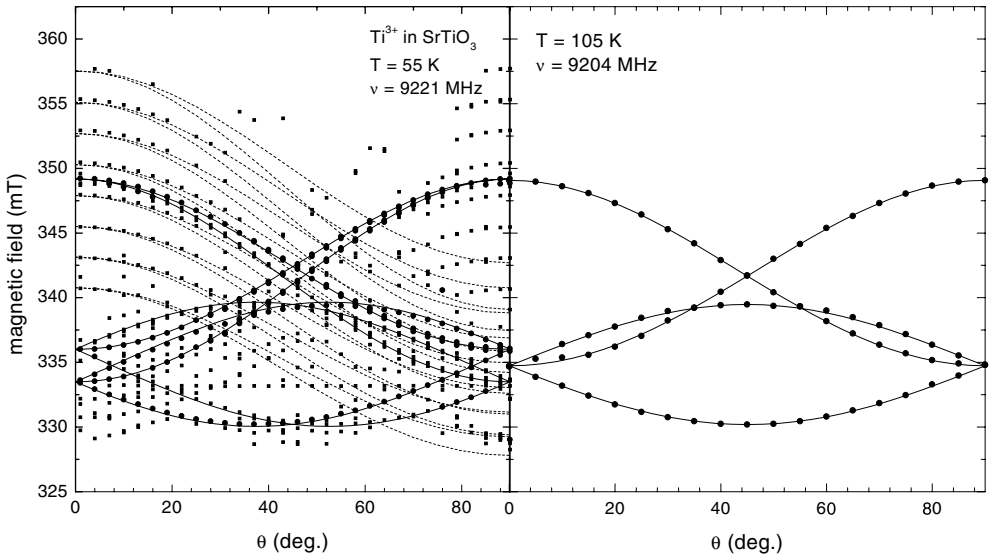

Figure 3. Angular dependences of Ti^{3+} resonance fields for a rotation of B in a (001) plane measured at $T = 55$ and 105 K. Smooth curves correspond to calculated $S = 1/2$, $I = 0$ resonances; dashed curves: $S = 1/2$, $I_1 = 5/2$, and $I_2 = 7/2$ hyperfine resonances for one of the centres.

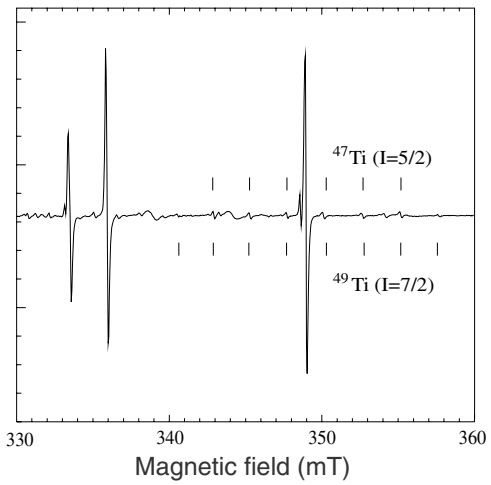

Figure 4. ^{47,49}Ti hyperfine structure, bracketing the ESR line of the $I = 0$ isotope of Ti^{3+} at $B \parallel [001]$; $T = 55$ K.

coincide with those of ^{49}Ti. The observed hyperfine structure quite clearly indicates that ESR spectra are caused by Ti-associated centres. The g-factor values indicate that we are dealing with Ti^{3+} ($3d^1$) ions.

There are 12 equivalent centres having the best resolution of their ESR lines at lower temperatures ($T < 80$ K). One of the principal axes of the Ti^{3+} exactly coincides with $\langle 001 \rangle$ crystal axes while the other two lie in the (001) plane and deviate from $\langle 110 \rangle$ crystal directions by the angle $\tau = \pm 8°$. For $T > 60$ K this deviation sharply decreases, finally vanishing at T close to T_c (figure 5). At the same time, the g-factor values describing ESR line positions

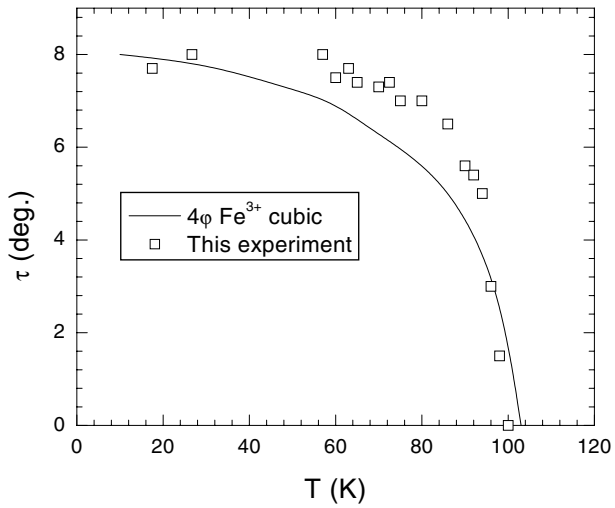

Figure 5. The temperature dependence of the orthorhombic Ti^{3+} rotation angle τ compared with that of cubic Fe^{3+}.

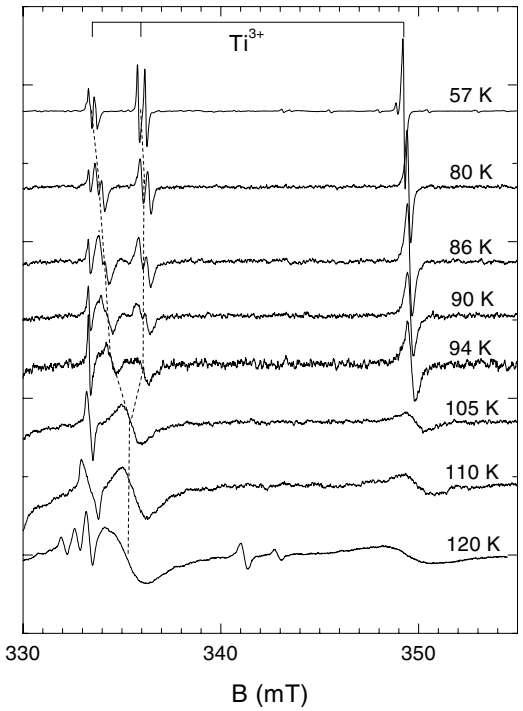

Figure 6. The ESR spectrum of Ti^{3+} taken at $B \parallel [001]$ for various temperatures.

as well as the orthorhombic symmetry of the centre remain practically unchanged at least up to 140–145 K where the spectrum could still be measured. As an illustration, in figure 6 we present the spectra taken at various temperatures. This figure also demonstrates broadening of the ESR lines with increasing temperature.

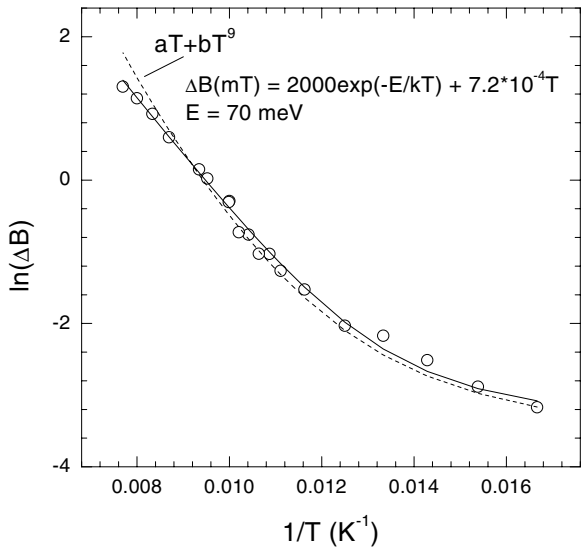

Figure 7. The temperature dependence of the ESR linewidth for Ti^{3+} at $B \parallel [001]$ (solid and dashed curves are calculated; circles are experimental data.)

At low temperatures ($T < 30$ K) the lines have predominant Gaussian shape with peak-to-peak width of only 0.05–0.06 mT. As the temperature increases, the ESR lines not only become broader but also their shape changes to Lorentzian, indicating a possibility of molecular motion between equivalent orthorhombic sites. The broadening between 30 and 140 K (figure 7) is satisfactorily fitted by

$$\Delta B \text{ (mT)} = 7.2 \times 10^{-4} T + 2000 \exp(-E/kT), \qquad E = 70 \text{ meV } (810 \text{ K}). \tag{2}$$

The first term in equation (2) is most probably connected with the spin–lattice relaxation contribution, namely the one-phonon (direct) process [12]. The second term, dominant at $T > 50$–60 K, is of thermally activated type. Its pre-exponential factor $1/\tau_0 = 2000$ mT $\approx 4 \times 10^{11}$ s^{-1} has a typical value often observed for rotation of paramagnetic complexes between equivalent positions. Note that this term cannot be related to the Orbach relaxation process usually observed for Ti^{3+} because, as follows from analysis of g-factor values (see section 3.4), all excited orbital states lie at a distance much larger than $E = 70$ meV ≈ 560 cm^{-1}. As an alternative mechanism for the contribution to the linewidth at $T > 50$ K, we considered two-phonon (Raman) process of the spin–lattice relaxation. In this case, the experimental data could not be so satisfactorily fitted by the function T^7—that, however, contradicts the T^9-law predicted for ions with an odd number of electrons [12]. In the following sections we will return to this problem once again.

3.3. Local structure of the Ti^{3+} centre

The ESR spectra of Ti^{3+} in $SrTiO_3$ have been previously observed in [7] and [8] and attributed to Ti^{3+} on Sr^{2+} sites. The Ti^{3+} centres described in this paper differ from those observed in [7] in g- and A-tensor values as well as in the orientation of their principal axes. We assume that the new Ti^{3+} ESR spectra arise from Ti^{3+} ions located in the regular Ti lattice sites. This assumption is based on the following experimental facts and arguments:

(i) The Ti^{3+} centres observed by us are created only by UV irradiation with an energy close to or larger than the forbidden gap of $SrTiO_3$, by capture of photoelectrons from the conduction band. Before UV irradiation these centres are completely absent. Figure 2 clearly shows that at each temperature where holes are thermally freed to the valence band, the intensity of Ti^{3+} decreases due to the partial recombination of holes on Ti^{3+} sites. Thus we can consider the Ti^{3+} centre as an electron donor with its energy level close to the bottom of the conduction band. At $T \approx 185$ K localized electrons are thermally excited to the conduction band and thereafter they can be recaptured by deeper centres and partly recombine with holes at Fe^{5+} sites, giving rise to the Fe^{3+} spectrum. Detailed analysis of the conditions of the Ti^{3+} creation as well as the processes of their destruction by temperature and infrared illumination irrefutably proves that electrons are freed at $T \approx 185$ K. On the other hand, the temperature stability of Fe^{5+} may occur at only slightly above 185 K, though there have been reports of stability of this centre up to room temperature [13].

The behaviour of Ti^{3+} in $SrTiO_3$ is very close to that in $PbTiO_3$ [2], where these centres are also created mainly by electron capture under light irradiation. The Ti^{3+} centres attributed to the Sr sites which were observed earlier [7] are thermally stable at room temperature and above. Moreover, neutron (electron) irradiation [7], or a corresponding high-temperature treatment, is needed for their creation.

(ii) The values of the hyperfine coupling tensor obtained from the experiment give additional support for our model. It is well known that the hyperfine interaction of a paramagnetic electron with a nucleus is very sensitive to the number of surrounding anions due to the covalence effect [12]. The hyperfine-tensor principal values described here are much larger than those reported for Ti^{3+} on Sr sites: $A_X = 13.5 \times 10^{-4}\,cm^{-1}$, $A_Y = 16.4 \times 10^{-4}\,cm^{-1}$, and $A_Z = 2.7 \times 10^{-4}\,cm^{-1}$ [7]. In contrast, these parameters are close to those found for Ti^{3+} in the orthorhombically distorted sixfold oxygen environment in $BaTiO_3$ [6].

(iii) The g-tensor axis orientation along $\langle 110 \rangle$ is distinctly different from that for the Ti^{3+} centres on Sr sites where the axis orientations are along (or close to) the cubic $\langle 001 \rangle$ directions.

Now let us discuss the origin of the orthorhombic symmetry of the Ti^{3+} centre and the mechanism of electron localization. There can be several possibilities for such a symmetry reduction of the centre.

(i) The orthorhombic symmetry of the Ti^{3+} centres can be attributed to the presence of either oxygen divacancy or a proton usually located between two oxygens [14]. Both of these defects are characteristic for the $SrTiO_3$ lattice. In an attempt to clarify such a possibility, high-temperature treatments in both inert-gas and oxygen atmospheres were performed. We did not find any correlation between the ESR intensity and the different treatment regimes. The ESR intensity did not change even upon annealing in the oxygen atmosphere, performed at 1150 °C for 20–22 h. These results mean that Ti^{3+} is related neither to oxygen vacancies nor to protons.

(ii) Another possibility for the orthorhombic symmetry could be Ca(Ba) ions located in the two Sr sites or, most probably, a positively charged interstitial ion between two Sr ions. From the symmetry point of view, such a position for an interstitial ion in the ABO_3 perovskite lattice is the most probable. However, the calculation of orbital energy levels of the Ti^{3+} performed on the basis of a point ion crystal-field approach clearly shows that the state $|xy\rangle$ remains a ground state in the presence of these defects. The $|xy\rangle$ ground state strongly contradicts observed g-factor shifts. For a d^1 ion, a g-value of ~ 2, as found for $g_{[110]}$ (1.9943), occurs only if the unpaired electron occupies an orbital such as $|3x_i^2 - r^2\rangle$ (here

$i = X, Y$, or Z) and if the external magnetic field B is oriented along the axis of this orbital. Significant reconstruction of the orbital energy structure can be expected for an off-centre position of the Ti^{3+} due to the possible influence of an impurity ion. This model is similar to that proposed by Muller and Blazey [15] to explain the orthorhombic Cr^{5+} spectrum of $SrTiO_3$, where the $3d^1$ electron ground state was assumed to be the $|3y^2 - r^2\rangle$ orbital (the orbital axis points along $\langle 110 \rangle$). Cr^{5+} was assumed to occupy an off-centre position with a displacement in the $\langle 110 \rangle$ direction. For a paramagnetic ion with an off-centre position in the oxygen octahedron, two g-tensor principal axes have to be rotated by the angle τ from the $\langle 110 \rangle$ axes, as is observed for both Cr^{5+} and Ti^{3+} at $T < T_c$. Obviously, the angle τ is determined by the value of the Cr^{5+} or Ti^{3+} shift. But this is not so in our case. At $T > T_c$, where the angle τ becomes zero, the Ti^{3+} has the same orthorhombic symmetry with the same g-factor values as at $T < T_c$. This means that the Ti^{3+} is an inversely symmetrical centre and its orthorhombicity results from orthorhombic distortion of the oxygen octahedron, i.e., the Ti^{3+} spectrum observed here may be due to the Jahn–Teller distortion with $T_{2g} \times (e_g + t_{2g})$ non-linear coupling. Therefore, our consideration of the Ti^{3+} spectrum should be rather analogous to that proposed by Glasbeek *et al* [16] for description of the orthorhombic Cr^{5+} in $SrTiO_3$. The model reported in [16] is based on a Jahn–Teller $T_{2g} \times (e_g + t_{2g})$ coupling and preceded the publication of Muller and Blazey [15].

We point out that in spite of some formal similarity of the Cr^{5+} and Ti^{3+} spectra, there is an essential difference between these two centres: Cr^{5+} is an impurity whereas the Ti^{3+} is created from a regular ion. Therefore, in the case of the Ti^{3+} ion, besides the explanation of its local symmetry we also need to find a mechanism leading to electron localization on the Ti^{4+} ion. Obviously a disturbing defect could be the main reason for electron localization on the Ti ion. If the reason were to be electron autolocalization like in $BaTiO_3$ [6], this centre should be observed in $SrTiO_3$ much earlier; however, many attempts to reveal these centres failed (see, for example, [17]).

Taking into account all arguments presented above, we propose the following model for the Ti^{3+} centre.

The Ti^{3+} centres are created on regular Ti sites closest to a disturbing defect (for definiteness we will assume an interstitial ion) located in the $\langle 110 \rangle$ directions by trapping the electron from the conduction band under UV irradiation. After being trapped, the electron is localized in one of the minima on the adiabatic potential energy surface of $T_{2g} \times (e_g + t_{2g})$ Jahn–Teller orthorhombic distortions. The energy minimum where the paramagnetic electron is located is lower than the others due to the influence of additional stress produced by an interstitial ion. Therefore, the $Ti^{3+} \rightarrow$ disturbing defect direction has to be the main axis of the Ti^{3+} centre. Obviously, there are four equivalent sites around an interstitial for the electron localization, as depicted in figure 8. It should be emphasized that instead of an interstitial ion, there could also be two Ba or Ca ions on Sr sites. According to this model together with the experimental facts presented, it is obvious that we are dealing with a Jahn–Teller system with rather strong localization of paramagnetic electrons in one of the distorted configurations. This follows from the fact that at least up to $T = 140$–150 K the system still exhibits a static Jahn–Teller effect. On the other hand, the observed exponential temperature broadening of ESR lines at $T > 60$ K speaks in favour of the presence of thermally activated hops of electrons from one distorted configuration to another. The activation energy ($E = 70$ meV) for such a hopping process is so big that it is comparable to the energy of Ti^{3+} thermal ionization (electrons freed from Ti^{3+} at $T \approx 185$ K). This could mean that the observed thermally activated process rather reflects an electron jump from one of the four Ti ions to another one located around a disturbing defect.

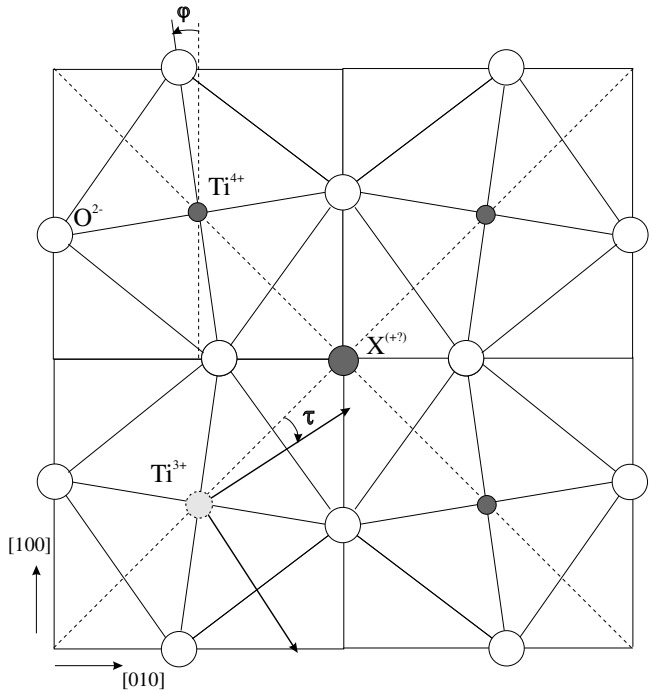

Figure 8. The model of the photoinduced Ti^{3+} centres in $SrTiO_3$.

The above-presented hypotheses relating to the Ti^{3+} centre were only qualitative. Further experiments as well as theoretical calculations are needed to support the model proposed. In the following, we give an analysis of g-factor values by considering the orbital-level splitting in the limit of a strong Jahn–Teller coupling.

3.4. Interpretation of the g-tensor

Some aspects should be elucidated by the calculation of the model of the centre. These are

(i) the symmetry of the centre and the orientation of the g-factor principal axes;
(ii) the nearly free electron value of $g_{[110]} = 1.992$.

As mentioned above, the symmetry of the centre may be explained by orthorhombic non-linear $T_{2g} \times (e_g + t_{2g})$ Jahn–Teller distortion of an oxygen octahedron. As shown in [20], in some cases the orthorhombic configuration can be more stable than pure tetragonal or trigonal distortions.

To simplify the g-factor calculation, we will consider the complex orthorhombic distortion to be a result of two simple Jahn–Teller static distortions. The first is a tetragonal distortion, in which the oxygen octahedron is stretched along the z-axis. It splits the t_{2g} manifold so that the energy of the $|d_{xy}\rangle$ state increases by Δ_{xy} (figure 9). The second, trigonal distortion,

$$\hat{H}_{trig} = -\delta(|\alpha\rangle\langle\alpha| - |\beta\rangle\langle\beta|), \tag{3}$$

removes the remaining degeneracy. Its eigenfunctions are

$$|\alpha\rangle \equiv (|d_{zy}\rangle + |d_{zx}\rangle)/\sqrt{2}, \qquad |\beta\rangle \equiv (-|d_{zy}\rangle + |d_{zx}\rangle)/\sqrt{2}. \tag{4}$$

The constant of the spin–orbit coupling

$$\hat{H}_{SO} \equiv \lambda \hat{L} \cdot \hat{S}$$

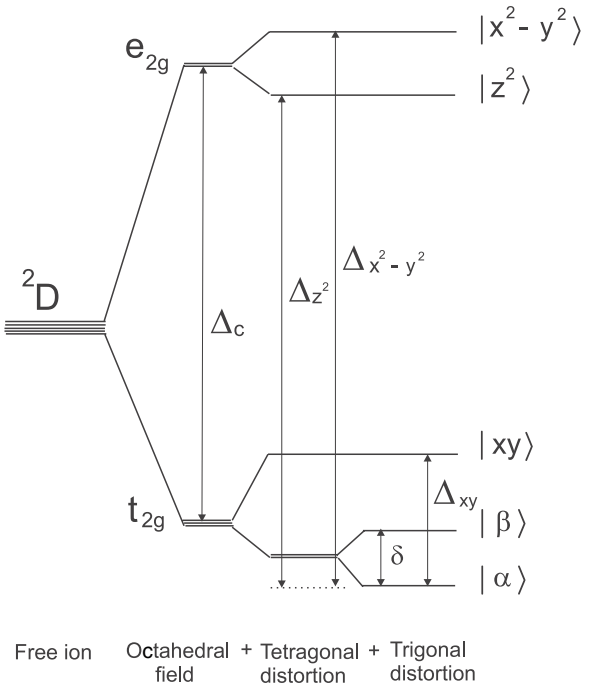

Figure 9. Splitting of the orbital states of a $3d^1$ ion in an octahedral field of a tetragonally stretched oxygen octahedron with added trigonal distortion.

is for the Ti^{3+} free ion $\lambda_0 \approx 154\ \mathrm{cm}^{-1}$. λ may be assumed small compared to Δ_{xy} and to the distance to the e_{2g} manifold Δ_c. We do not *a priori* know the ratio λ/δ and will consider $\hat{H} = \hat{H}_{trig} + \hat{H}_{SO}$ as the zeroth-order Hamiltonian. The Hamiltonian matrix is

$$\begin{pmatrix} -\delta & \mathrm{i}\lambda/2 \\ -\mathrm{i}\lambda/2 & \delta \end{pmatrix}. \tag{5}$$

The ground state Kramers doublet

$$\begin{aligned} |G\rangle &= (\cos\phi)|\alpha\uparrow\rangle + \mathrm{i}(\sin\phi)|\beta\uparrow\rangle \\ |G^*\rangle &= (\cos\phi)|\alpha\downarrow\rangle + \mathrm{i}(\sin\phi)|\beta\downarrow\rangle \end{aligned} \tag{6}$$

has principal values of the g-factor

$$\begin{aligned} g_{[001]} &= g_s - 2\sin 2\phi, \\ g_{[110]} &= g_s\cos 2\phi - 2\lambda\left(\frac{\sin^2\phi}{\Delta_{xy}} + \frac{3\sin^2\phi}{\Delta_{z^2}} + \frac{\cos^2\phi}{\Delta_{x^2-y^2}}\right), \\ g_{[\bar{1}10]} &= g_s\cos 2\phi - 2\lambda\left(\frac{\cos^2\phi}{\Delta_{xy}} + \frac{3\cos^2\phi}{\Delta_{z^2}} + \frac{\sin^2\phi}{\Delta_{x^2-y^2}}\right), \end{aligned} \tag{7}$$

where $\tan 2\phi = \lambda/2\delta$.

We see that the model gives the correct g-factor symmetry. The ratio λ/δ may be extracted from $g_{[001]}$:

$$2\sin 2\phi = g_s - g_{[001]} = 0.118,$$

which gives $\delta \approx 900\ \mathrm{cm}^{-1}$ for $\lambda = 110\ \mathrm{cm}^{-1}$. Here $\lambda = k\lambda_0$, where the factor $k \simeq 0.7$ takes into account covalence effects. We see that, in fact, the spin–orbit interaction is much

smaller than the energy splitting caused by trigonal distortion and cannot compete with Jahn–Teller instability. The energy splittings Δ_{xy}, Δ_{z^2}, $\Delta_{x^2-y^2}$ were calculated from the other two g-factors using equations (7). They are: $\Delta_{xy} \simeq 6500\ \mathrm{cm}^{-1}$, $\Delta_{z^2} \simeq 23\,000\ \mathrm{cm}^{-1}$, $\Delta_{x^2-y^2} \simeq 30\,000\ \mathrm{cm}^{-1}$. All energy splittings obtained have reasonable values for $SrTiO_3$ structure. Further, using the energy splittings we can estimate the magnitude of the tetragonal distortion (s) of an oxygen octahedron. This was done by adopting the Harrison parametrization scheme [21] for an electronic structure calculation. This gives a reasonable value for an oxygen octahedron stretch: $s \approx 0.15$–0.17 Å.

Finally, we briefly discuss an orthorhombic Cr^{5+} ion in $SrTiO_3$ whose spectral parameters are close to those of the Ti^{3+} described by us. We have to pay attention to the measurement of the electric dipole moment associated with the off-centre Cr^{5+} ion within the oxygen octahedron [22]. From $qd = 0.18q$ Å, an off-centre displacement of about 0.04 Å (charge $q = 5e$) was determined for Cr^{5+} ions. Since Cr^{5+} becomes quasi-tetrahedrally coordinated by four O^{2-} ions in the perovskite lattice (note: the Ti^{4+}–O^{2-} distance in the TiO_6 octahedron is $\sim$2 Å), a displacement of 0.09 Å can be considered to be too small. Furthermore, in the interpretation of the effect of an external electric field on a paramagnetic ion in the $SrTiO_3$ lattice, the electrostriction coupling becoming anomalously strong at low temperatures should be taken into account. In this case, the effect of an electric field on a paramagnetic ion may be equivalent to the effect of uniaxial stress. Thus it does not contradict possible Jahn–Teller orthorhombicity of Cr^{5+}. Obviously, a detailed theoretical calculation of the electronic structure and additional experiments (for example, measurements of dielectric losses, which are very sensitive to the presence of electric dipoles in the lattice) would be desirable to clarify the model of the Cr^{5+} centre.

4. Conclusions

(1) We revealed a new Ti^{3+} centre in pure $SrTiO_3$ crystals created by UV irradiation at low temperatures ($T < 180$ K). At $T > T_c$ ($T_c \simeq 105$ K corresponds to the temperature of the cubic–tetragonal phase transition) the Ti^{3+} centre exhibits an orthorhombic symmetry of the g-tensor with its principal axes oriented exactly along $\langle 001 \rangle$ and $\langle 110 \rangle$ crystal directions. At $T < T_c$, due to a phase transition, two of the principal axes of the Ti^{3+} are tilted from the $\langle 110 \rangle$ directions by $\pm 8^\circ$ in (001) crystal plane.

(2) On the basis of analysis of the g-factor and the values of the ^{47,49}Ti hyperfine splitting, we concluded that the Ti^{3+} centres are created in slightly perturbed regular Ti^{4+} sites by trapping a photoelectron from the conduction band. Trapped electrons are thermally excited back to the conduction band at $T \gtrsim 180$ K.

(3) The spectroscopic data (g-factors and the symmetry of the centre) were explained assuming a Jahn–Teller orthorhombic distortion of an oxygen octahedron with strong $T_{2g} \times (e_g + t_{2g})$ non-linear vibronic coupling.

References

[1] Possenriede E, Jacobs P and Schirmer O F 1992 *J. Phys.: Condens. Matter* **4** 4719
[2] Laguta V V, Glinchuk M D, Bykov I P, Maksimenko Yu L, Rosa J and Jastrabík L 1996 *Phys. Rev.* B **54** 12353
[3] Muller K A, Berlinger W and Rubins R S 1969 *Phys. Rev.* **186** 361
[4] Schirmer O F, Berlinger W and Muller K A 1975 *Solid State Commun.* **16** 1289
[5] Berney R L and Cowan D L 1981 *Phys. Rev.* B **23** 37
[6] Scharfschwerdt R, Mazur A, Schirmer O F, Hesse H and Mendricks S 1996 *Phys. Rev.* B **54** 15284
[7] Schirmer O F and Muller K A 1973 *Phys. Rev.* B **7** 2986
[8] Blazey K W, Koch R and Muller K A 1981 *Mater. Res. Bull.* **16** 1149

[9] Kool Th W and Glasbeek M 1993 *J. Phys.: Condens. Matter* **5** 361
[10] Blazey K W, Schirmer O F, Berlinger W and Muller K A 1975 *Solid State Commun.* **16** 1289
[11] Muller K A, Waldkirch Th and Berlinger W 1971 *Solid State Commun.* **9** 1097
[12] Geschwind S (ed) 1972 *Electron Paramagnetic Resonance* (New York: Plenum)
[13] Ensing T S and Stokowski S E 1970 *Phys. Rev.* B **1** 2799
[14] Sata N, Hiramoto K, Ishigame M, Hosoya S, Niimura N and Shin S 1996 *Phys. Rev.* B **54** 15795
[15] Muller K A and Blazey K W 1993 *Solid State Commun.* **85** 381
[16] Glasbeek M, de Jong H J and Koopmans W E 1979 *Chem. Phys. Lett.* **66** 203
[17] Muller K A, Berlinger W and Rubins R S 1969 *Phys. Rev.* **186** 361
[18] Abragam A and Bleaney B 1970 *Electron Paramagnetic Resonance of Transition Ions* (Oxford: Clarendon)
[19] Davies J J and Wertz J E 1969 *J. Magn. Reson.* **1** 500
[20] Bersuker I B and Polinger V Z 1973 *Phys. Lett.* A **44** 495
[21] Harrison W A 1980 *Electronic Structure and the Properties of Solids* (San Francisco, CA: Freeman)
[22] Kool Th W, de Jong H J and Glasbeek M J 1994 *J. Phys.: Condens. Matter* **6** 1571